Engineering Geology 105 (2009) 200–210

Contents lists available at ScienceDirect

Engineering Geology

journal homepage: www.elsevier.com/locate/enggeo

Estimating earthquake hazard parameters from instrumental data for different regions in and around Turkey

Yusuf Bayrak [a,*], Serkan Öztürk [a], Hakan Çınar [a], Doğan Kalafat [b], Theodoros M. Tsapanos [c], G. Ch. Koravos [c], G.-A. Leventakis [c,1]

[a] Karadeniz Technical University, Department of Geophysics, 61080 Trabzon, Turkey
[b] Boğazici University, Kandilli Observatory and Earthquake Research Institute, 34684, İstanbul, Turkey
[c] Aristotle University of Thessaloniki, School of Geology, Geophysical Laboratory, 54124, Thessaloniki, Greece

ARTICLE INFO

Article history:
Received 4 June 2008
Received in revised form 30 January 2009
Accepted 11 February 2009
Available online 21 February 2009

Keywords:
Maximum magnitude $\hat{M}_{max}$
$\hat{b}$ value
Mean activity rate $\hat{\lambda}$
Index K
Earthquake hazard

ABSTRACT

We conducted a study of the spatial distributions of seismicity and earthquake hazard parameters for Turkey and the adjacent areas, applying the maximum likelihood method. The procedure allows for the use of either historical or instrumental data, or even a combination of the two. By using this method, we can estimate the earthquake hazard parameters, which include the maximum regional magnitude $\hat{M}_{max}$, the activity rate of seismic events and the well-known $\hat{b}$ value, which is the slope of the frequency-magnitude Gutenberg-Richter relationship. These three parameters are determined simultaneously using an iterative scheme. The uncertainty in the determination of the magnitudes was also taken into consideration. The return periods (RP) of earthquakes with a magnitude $M \geq m$ are also evaluated. The whole examined area is divided into 24 seismic regions based on their seismotectonic regime. The homogeneity of the magnitudes is an essential factor in such studies. In order to achieve homogeneity of the magnitudes, formulas that convert any magnitude to an M_S-surface scale are developed. New completeness cutoffs and their corresponding time intervals are also assessed for each of the 24 seismic regions. Each of the obtained parameters is distributed into its respective seismic region, allowing for an analysis of the localized seismicity parameters and a representation of their regional variation on a map. The earthquake hazard level is also calculated as a function of the form $\Theta = (\hat{M}_{max}, RP_{6.0})$, and a relative hazard scale (defined as the index K) is defined for each seismic region. The investigated regions are then classified into five groups using these parameters. This classification is useful for theoretical and practical reasons and provides a picture of quantitative seismicity. An attempt is then made to relate these values to the local tectonics.

© 2009 Elsevier B.V. All rights reserved.

1. Introduction

Several local and regional seismic hazard studies (Aslan, 1972; Båth, 1979; Yarar et al., 1980; Erdik et al., 1999; Kayabalı and Akın, 2003; Bayrak et al., 2005) have been performed in order to estimate the seismic hazard in Turkey using the statistical processing of instrumental earthquake data. Although many reports show that Turkish instrumental records are far from incomplete for a probabilistic approach to seismic hazard, a serious effort is undertaken here for such analysis. We applied a procedure developed by Kijko and Sellevoll (1989; 1992). The proposed approach is very flexible and provides several attractive properties. It accommodates "gaps" in both historical and complete parts of the catalog. It makes it possible to estimate the maximum regional magnitude $\hat{M}_{max}$ from the largest historical known earthquake, which occurred before catalogs begin. It allows for the combination of earthquakes of the historical epoch and those extracted from short periods of instrumental data. The complete part of the catalog can be divided into time intervals of different levels of completeness. An illustration of the quality of the data, which can be used to obtain the seismic parameters through this approach, can be seen in Kijko and Sellevoll (1992).

In the present study, a method for estimating $\hat{M}_{max}$ and other related parameters such as the magnitude-frequency relationship $\hat{\beta}$ and the mean seismic activity rate $\hat{\lambda}$ introduced by Kijko and Sellevoll (1989) is applied. We applied maximum likelihood estimation in Turkey and the adjacent areas on the basis of a procedure that uses data from both incomplete and complete files. The computations of the method are based on the assumption that earthquakes have a Poisson occurrence over time with a mean activity rate λ and a doubly truncated frequency-magnitude Gutenberg–Richter relation. The standard deviations of these parameters are also estimated. The mean return periods (RP) of earthquakes with a certain magnitude $M \geq m$ are determined.

* Corresponding author. Tel.: +90 462 3772026; fax: +90 462 3257405.
E-mail address: bayrak@ktu.edu.tr (Y. Bayrak).
[1] Deceased.

0013-7952/$ – see front matter © 2009 Elsevier B.V. All rights reserved.
doi:10.1016/j.enggeo.2009.02.004

2. Tectonic settings

Turkey is located in the Mediterranean part of Alpine–Himalayan orogenic system, which strikes in a mean west-east direction from the Mediterranean to Asia. The tectonic regime of Turkey and its vicinity is controlled by three major plates: the African, Eurasian and Arabian. Two minor plates also exist, the Aegean and Anatolian, as shown in the neotectonic models of McKenzie (1972) and Dewey et al. (1973). The Aegean Arc, the West Anatolian Graben Complexes (WAGC), the North Anatolian Fault Zone (NAFZ), the East Anatolian Fault Zone (EAFZ), the North East Anatolian Fault Zone (NEAFZ), the Bitlis Thrust Zone (BTZ), and the Caucasus represent the most important tectonic features of Turkey, as shown in Fig. 1 (adopted from Şaroğlu et al. (1992) and Ulusay et al. (2004)).

The Arabian and Eurasian plates collide along the Bitlis Thrust Zone (Şengör and Yılmaz, 1981), resulting in the uplift of mountains along the suture. The Bitlis Suture is a complex continent-continent and continent-ocean collisional boundary that lies north of the fold-and-thrust belt of the Arabian platform and extends from southeastern Turkey to the Zagros Mountains in Iran (Bozkurt, 2001). GPS velocities for the Bitlis Thrust Zone on the northern edge of the Arabian plate indicate a NW-oriented motion of 18 ± 2 mm/yr relative to Eurasia (McClusky et al., 2000). The convergence between the Arabian and Eurasian plates pushes the Anatolian Plate westward along the NAFZ and EAFZ. The NAFZ and EAFZ constitute the northern and southern boundaries of this plate, respectively, although the southern boundary is not well defined by seismicity.

The North Anatolian Fault Zone is one of the best-known dextral strike-slip faults in the world because of its remarkable seismic activity, extremely well-developed surface expression and importance for the tectonics of the eastern Mediterranean region. The NAFZ is a very active structure, and according to geodesy it accommodates 24–30 mm/yr of dextral motion (Reilinger et al., 1997). The NAFZ is an approximately 1500 km-long, broadly arc-shaped, dextral strike-slip fault system that extends from eastern Turkey in the east to the north Aegean in the west. It is predominantly a single zone of a few hundred meters to 40 km wide. Along much of its length, this fault zone consists of a few shorter sub-parallel fault strands that sometimes display an anastomosing pattern (Bozkurt, 2001). To the east, the NAFZ forms a typical triple-junction and joins with the sinistral East Anatolian Fault Zone at Karlıova. The NAFZ does not terminate at the Karlıova triple junction, but continues towards the southeast.

The East Anatolian Fault Zone is a 550 km-long, approximately northeast-trending, sinistral strike-slip fault zone that comprises a series of faults arranged parallel, sub-parallel or obliquely to the general trend (Bozkurt, 2001). Computations from GPS data (McClusky et al., 2000) reveal sinistral motion equal to $9 + 2$ mm/yr in the EAFZ. The zone is a transform fault forming parts of boundaries between the Anatolian and the Eurasian plates and between the Arabian and African plates. It is considered a conjugate structure to the NAFZ. The left-lateral slip along the fault zone contributes to the westward extrusion of Anatolia. The structure of the fault zone is complicated, with several pull-apart basins, conjugate fractures, folding, and a considerable thrust component.

The area to the east of the Karlıova triple junction is characterized by a N–S compressional tectonic regime. Conjugate strike-slip faults of dextral and sinistral character paralleling the North and East Anatolian fault zones dominate the region (Bozkurt, 2001). These structures include the Çaldıran Fault, Erciş Fault, Iğdır Fault, Malazgirt Fault, Süphan Fault, Kağızman Fault Zone, Tutak Fault Zone and Northeast Anatolian Fault Zone (Fig. 1). Although the conjugate strike-slip fault system dominates the active tectonics of eastern Anatolia, the E–W-trending basins of compressional origin form the most spectacular structures of the region as they indicate N–S convergence and shortening of the Anatolian plateau (Wong et al., 1978). The GPS data give 10 ± 2 mm/yr for the total shortening between the strike-slip faults in eastern Turkey and thrusting along the Caucasus (McClusky et al., 2000).

The Cyprean Arc is considered the presently active plate boundary that accommodates the convergence between the African plate to the south and the Anatolian Plate to the north, in the eastern Mediterranean. Northeastward subduction (west of Cyprus) of the eastern Mediterranean oceanic crust has been proposed to take place on the basis of earthquake

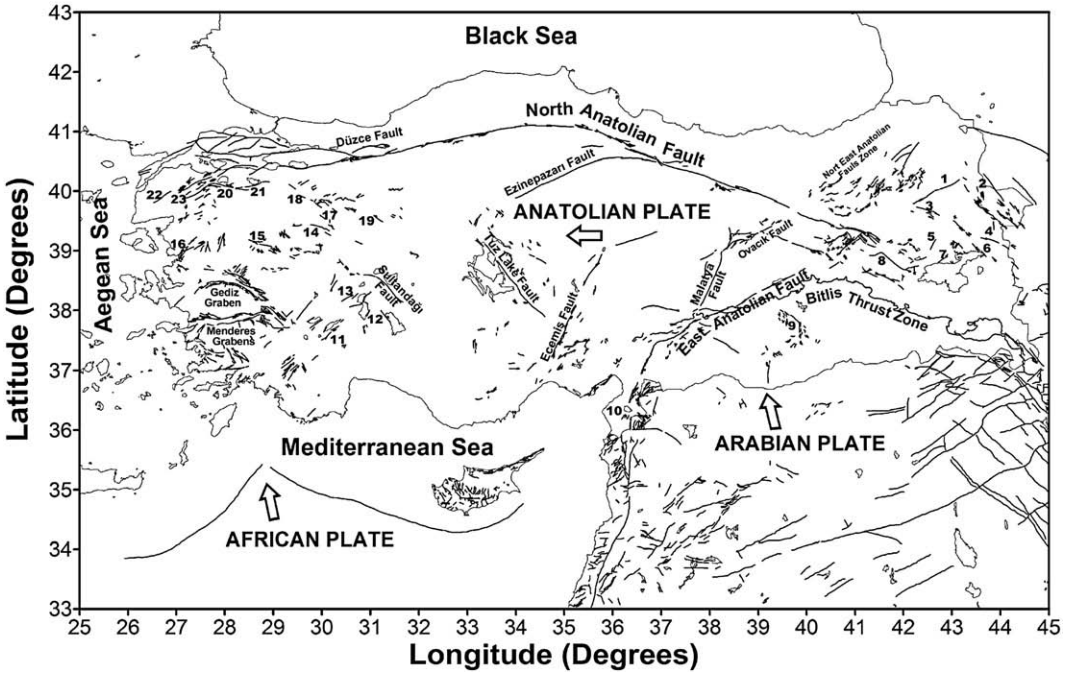

Fig. 1. Active fault map of Turkey. The major tectonic structures are modified from Şaroğlu et al. (1992) and Ulusay et al. (2004). (Names of numbered faults; 1: Kağızman, 2: Iğdır, 3: Tutak, 4: Çaldıran, 5: Malazgirt, 6: Erciş, 7: Süphan, 8: Muş Thrust Zone, 9: Karacadağ Extension Zone, 10: Junction of a part of Dead Sea fault and EAFZ, 11: Burdur Fault Zone, 12: Beyşehir, 13: Tatarlı, 14: Kütahya, 15: Simav, 16: Zeytindağ–Bergama, 17: Eskişehir, 18: İnönü–Dodurga, 19: Kaymaz, 20: Manyas, 21: Ulubat and 22: Etili.

data and on the assumption of the continuation of the plate boundary from the Aegean arcs. Based on seismicity, the main area of active convergence extends from Cyprus to the İskenderun Bay toward the Kahramanmaraş triple junction, where the East Anatolian and the Dead Sea Fault Zones (DAFZ) cross each other (Bozkurt, 2001).

The Dead Sea Transform Fault Zone is a 1000 km-long, approximately N–S-trending, sinistral intraplate strike-slip fault zone. Its internal structure is dominated by left stepping *en échelon* strike-slip faults separated by pull-apart basins or rhomb grabens (Bozkurt, 2001). In terms of plate tectonics, the DSFZ is considered to be a transform plate boundary, separating the African Plate to the west and the Arabian Plate to the east (Şengör and Yılmaz, 1981). The Arabian Plate is moving northward faster than the African Plate. This differential movement between the plates is taken up by DSFZ.

Convergence between the African and Anatolian plates in the Eastern Mediterranean takes place by subduction along the Aegean and Cyprus arcs (Papazachos and Comninakis, 1971; Mart and Woodside, 1994). The African Plate is descending beneath the Anatolian Plate in a north-northeast direction. The Aegean arc system plays an important role in the geodynamical evolution of the Aegean region. The nature and structure of the trench is variable across the Aegean Arc. The eastern part acts rather as transform fault. Several trenches have been distinguished along the eastern parts of the Aegean Arc (Le Pichon and Angelier, 1979). The central and southern Aegean is characterized by coherent motion (internal deformation of <2 mm/yr) toward the SW at 30 ± 1 mm/yr relative to Eurasia (McClusky et al., 2000).

Western Anatolia forms one of the most seismically active and rapidly extending regions in the world, with currently an approximate N–S continental extension rate of 30–40 mm/yr (Oral et al., 1995; Le Pichon et al., 1995). Approximately E–W-trending grabens (e.g., Edremit, Bakırçay, Kütahya, Simav, Gediz, Küçük Menderes, Büyük Menderes, and Gökova grabens) and their basin-bounding active normal faults are the most prominent neotectonic features (Mckenzie, 1978; Le Pichon and Angelier, 1979). In western Turkey, the seismicity related to the West Anatolian Graben Complexes is high and generally displays swarm-type activity with a remarkable clustering of low-magnitude earthquakes in time and space (Üçer et al., 1985; Eyidoğan, 1988). However, large earthquakes sometimes occur in this region because of stresses resulting from sink basins, such as the Demirci ($M_S = 6.0$), Alaşehir ($M_S = 6.6$) and Gediz ($M_S = 7.0$) earthquakes (Eyidoğan, 1988). Eyidoğan and Jackson (1985) did a seismological study of the Demirci, Alaşehir and Gediz earthquakes of 1960–1970. Their interpretation of the faulting in the Gediz and Alaşehir earthquakes involves flattening of the fault planes below the brittle upper layer of the crust, at depths of 6–10 km but whose precise position is controlled by the temperature gradient. They stated that the source dimensions of these earthquakes were only three or four times the brittle crustal thickness. Such long-period detachment signals have been observed elsewhere, notably in the 1980 El Asnam earthquake, which involved thrust faulting (Eyidoğan and Jackson, 1985).

3. Seismic source zones and data

A seismic source zone is defined as a seismically homogeneous area. A complete understanding of the historical and instrumental seismicity, tectonics, geology, paleoseismology, and other neotectonic properties of the considered region are necessary for an ideal delineation of seismic source zones. However, it is not always possible to compile detailed information in all of these fields for the majority of the world. Thus, seismic source zones are frequently determined using two fundamental tools: the seismicity profile and the tectonic structure of the region under consideration (Erdik et al., 1999). Several authors have suggested that seismic source zonation is a widely used methodology to determine earthquake hazard and have performed numerous studies. However, although seismic source zonation is a widely used methodology for determining earthquake hazards, it is not the only approach. Since delineating seismic zones still remains somewhat subjective, some researchers have suggested many different methods for evaluating seismic hazard. This is particularly important in areas where the tectonic structure is fragmented and the seismic activity is diffuse. For example, Alptekin (1978) developed an extensive study to calculate the Gutenberg–Richter regression constants of all Turkey events for the period 1900 to 1961. He determined 13 distinct zones in and around Turkey. Erdik et al. (1999) defined 37 source zones using all the available data and considering the studies and zonations presented by other researchers. Bayrak et al. (2005) divided Turkey into eight different source regions in order to estimate seismic hazard parameters, taking into consideration the environments and epicenters of earthquakes. A total of 14 seismic sources were delineated in Turkey by Kayabalı (2002). Based on the aforementioned studies, seismic source zones determined in this study were delineated mostly based on the Erdik et al. (1985), Yaltırak et al. (1998) and Kayabalı (2002) studies.

Plotting the existing tectonic structure with the distribution of earthquakes epicenters, and taking into account the solutions of focal mechanism given by the Scientific and Technological Research Council of Turkey (TUBITAK) for the great earthquakes that occurred in Turkey from 1977 to 2002, Turkey and its adjacent areas are divided in 24 different source regions. One of the objectives of this study is to compare the tectonics with the earthquake hazard, and for this a large number of data are needed. For this reason, we believe that smaller regions mostly contain insufficient data for further analysis. The seismic zones from 1 to 19, which include the easternmost part of Turkey and the Cyprus, Aegean and Mediterranean regions, were modified based on Erdik et al. (1999). In order to construct new zonations for the NAFZ including the source regions 20, 21, and 24, we took the studies by Alptekin (1978), Erdik et al. (1999), Jiménez et al. (2001) and Kayabalı (2002) into consideration. The rest of the source regions (22 and 23) were modified in accordance with the zonations by Erdik et al. (1999). The seismic source zones are shown in Fig. 2. The seismic source regions numbered from 1 to 24 are given as follows:

Zone 1) Northeast Anatolian Fault Zone (NEAFZ)
Zone 2) Kağızman, Iğdır, Tutak and Çaldıran faults (KITÇF)
Zone 3) Malazgirt, Erciş and Süphan faults and Muş Thrust Zone (MESF)
Zone 4) Bitlis Thrust Zone (BTZ)
Zone 5) Karacadağ Extension Zone (KEZ)
Zone 6) East Anatolian Fault Zone (EAFZ)
Zone 7) Junction of A part of Dead Sea Fault and EAFZ
Zone 8) Northern part of Cyprus
Zone 9) Southern part of Cyprus, including eastern part of Cyprus Arc
Zone 10) Western part of Cyprus Arc
Zone 11) Muğla and Rhodes
Zone 12) Aegean Arc
Zone 13) Burdur Fault Zone (BFZ)
Zone 14) Büyük and Küçük Menderes Grabens
Zone 15) Gediz Graben
Zone 16) Sultandağı, Beyşehir and Tatarlı faults (SBTF)
Zone 17) Kütahya, Simav and Zeytindağ–Bergama faults (KSZBF)
Zone 18) Eskişehir, İnönü–Dodurga and Kaymaz faults (EİDKF)
Zone 19) Yenice–Gönen, Manyas, Ulubat and Etili faults (YGMUEF)
Zone 20) Marmara part of North Anatolian Fault Zone (MNAFZ)
Zone 21) Anatolian part of North Anatolian Fault Zone (ANAFZ)
Zone 22) Mid–Anatolian Fault System (MAFS)
Zone 23) Ovacık fault and Malatya fault (OMF)
Zone 24) Eastern part of North Anatolian Fault Zone (ENAFZ)

In the early 1900s, when the instrumental period started in Turkey, only a few seismic stations existed. Therefore, recorded shocks during

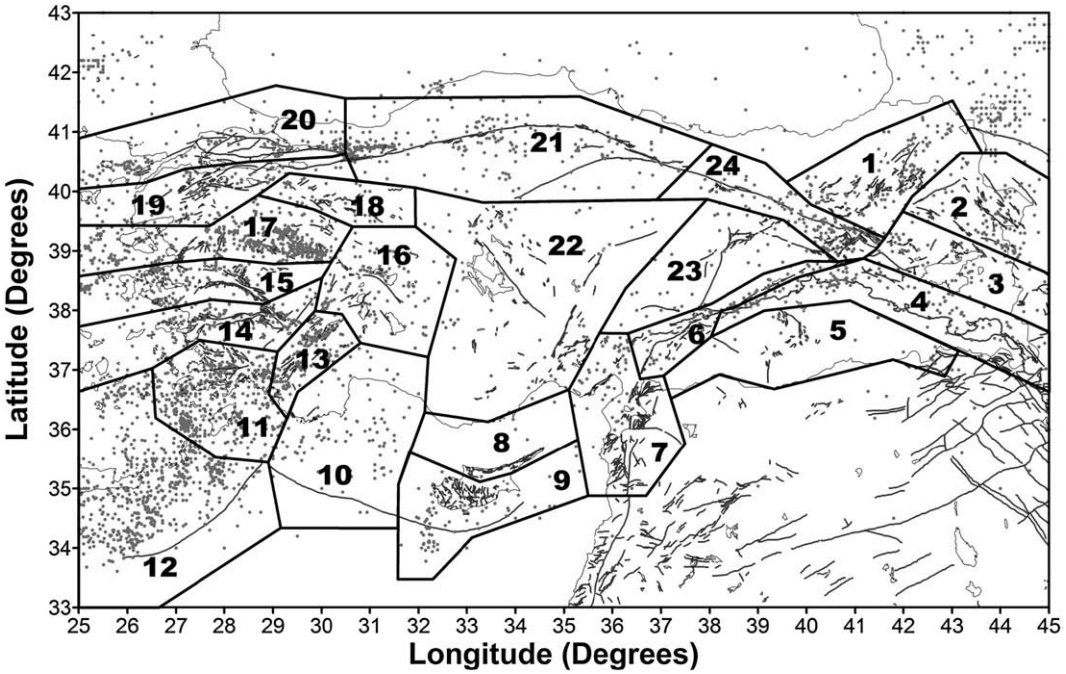

Fig. 2. Seismic source zones considered in this study together with the major tectonic features. The geographical distributions of earthquakes of M_S between 4.0 and 8.0 for the time period 1900–2005 are also shown.

that epoch are limited for the first half of the instrumental period. With the increasing number of stations installed around the 1970s, the second half of the instrumental period provides record events in all of the tectonic provinces of Turkey. Temporal changes in the number of earthquakes per year point out that the recorded values (earthquake magnitudes) within the first half of the instrumental period are lower than in the second half, for the aforementioned reason. Thus, the distribution of earthquakes that occurred during the second half of the instrumental period was examined in detail, in order to avoid misinterpreting the temporal changes in seismic activity in Turkey. Erdik et al. (1999) stated that the seismic activity gradually increased after 1965, reaching a maximum between 1970 and 1984, with a decreasing trend afterwards.

The database analyzed in this study is compiled from different sources, and the seismicity data come from different catalogs with different magnitude scales. The Turkey earthquake catalog, taken from the Bogaziçi University, Kandilli Observatory and Earthquake Research Institute (KOERI) and covering the period 1974 to 2005, contains 68478 events. The earthquakes from 1900 to 1974, which come from the International Seismological Centre (ISC) and instrumental catalog of KOERI, include 2398 events. The catalog contains the origin time, different magnitude scales (m_b — body wave magnitude, M_S — surface wave magnitude, M_L — local magnitude, M_D — duration magnitude, and M_W — moment magnitude), epicenters and depth information of the earthquakes. Moreover, earthquakes whose magnitudes are not given in the KOERI catalogue are completed from the different national and international catalogues, such as the General Directorate of Disaster Affairs Earthquake Research Department (TURKNET, Seismology Department), International Seismological Centre (ISC), and Incorporated Research Institutions for Seismology (IRIS) and Scientific and Technological Research Council of Turkey (TUBITAK) catalogs. Earthquakes with missing magnitudes have been added to the KOERI catalog from several websites, including that of TURKNET for 1991–2005, ISC for 1900–2002, IRIS catalog for 1974–2005, and TUBITAK for 1900–2005. Thus, the final data catalog consists of 70876 earthquakes with magnitudes greater than or equal to 1.0. Further analysis was carried out in a rectangular area between 25°E and 45°E in longitude and 33°N and 43°N in latitude. Thus, the magnitudes in the final catalog are M_S — surface wave magnitude. The time interval considered for the present work was 1900 to 2005. This study is restricted to shallow earthquakes (depth<60 km) and consists of 69339 events.

The earthquake data from the different catalogs are provided in different scales. For many earthquakes, there is more than one magnitude value, sometimes in different magnitude scales. Sn earthquake dataset used to assess earthquake hazard must be homogeneous, in other words the same magnitude scale must be used. In order to construct a homogeneous earthquake catalog, some new relationships must be developed among the different magnitude scales (m_b, M_S, M_L, and M_D) for the 24 different regions of Turkey. Principal components analysis can be used to fit a linear regression that minimizes the perpendicular distances from the data to the fitted model. The orthogonal regression method is applied for the fitting procedure, because the standard least squares method is based on the assumption that the values on a horizontal axis are estimated without error. Orthogonal regression is one of the most common techniques for errors-in-variables estimation in the simple linear regression model. It is sometimes known as the functional maximum likelihood estimator under the constraint of the known error variance ratio (Carroll and Ruppert, 1996). This is the linear case of what is known as orthogonal regression or total least squares, and is appropriate when there is no natural distinction between predictor and response variables, or when all variables are measured with error. This is in contrast to the usual regression assumption, where the predictor variables are measured exactly, and only the response variable has an error component. In this study, both regression methods are applied to the data of region 1 in order to show the differences between the fits. The orthogonal regression fits are listed in Table 1 and the uncertainty values are given in the parentheses. Also, the correlation coefficients (r) of all fits are given in Table 1. No relationship was calculated for regions with fewer than ten earthquakes. Consequently, using the relations given in Table 1, we constructed a uniform catalog of M_S.

As shown in the epicentral distribution of earthquakes in Fig. 3, there are four earthquakes with magnitudes $M_S \geq 7.5$. The largest earthquakes in the catalog are: 1926 Rhodes, $M_S = 7.7$; 1939 Erzincan, $M_S = 7.9$; 1976 Çaldıran–Muradiye (Van), $M_S = 7.5$ and 1999 İzmit,

Table 1
Relationships between different magnitude scales for 24 different source regions of Turkey.

Region number	Earthquakes number	Calculated relationships	Correlation coefficient (r)
1	52	$M_S = 1.643(\pm 0.184) * m_b - 3.258(\pm 0.404)$	0.778
2	26	$M_S = 1.844(\pm 0.275) * m_b - 4.138(\pm 0.605)$	0.796
3	13	$M_S = 1.306(\pm 0.364) * m_b - 1.876(\pm 0.792)$	0.705
4	56	$M_S = 1.973(\pm 0.296) * m_b - 4.457(\pm 0.635)$	0.665
5	12	$M_S = 0.748(\pm 0.126) * m_b - 0.949(\pm 0.272)$	0.863
6	30	$M_S = 1.447(\pm 0.196) * m_b - 2.187(\pm 0.423)$	0.803
7	23	$M_S = 1.842(\pm 0.268) * m_b - 4.394(\pm 0.588)$	0.820
8	2	–	–
9	35	$M_S = 1.578(\pm 0.292) * m_b - 2.956(\pm 0.648)$	0.674
10	40	$M_S = 1.429(\pm 0.252) * m_b - 2.242\ (\pm 0.548)$	0.667
11	167	$M_S = 0.810(\pm 0.071) * m_b - 0.682(\pm 0.150)$	0.661
12	263	$M_S = 0.997(\pm 0.079) * m_b - 0.146(\pm 0.167)$	0.614
13	23	$M_S = 2.168(\pm 0.680) * m_b - 5.326(\pm 1.430)$	0.554
14	51	$M_S = 0.997(\pm 0.167) * m_b - 0158(\pm 0.352)$	0.641
15	135	$M_S = 0.930(\pm 0.056) * m_b + 0.278(\pm 0.116)$	0.817
16	17	$M_S = 1.425(\pm 0.489) * m_b - 1.819(\pm 1.003)$	0.577
17	206	$M_S = 0.913(\pm 0.051) * m_b + 0.326(\pm 0.103)$	0.783
18	10	$M_S = 1.891(\pm 1.470) * m_b - 3.574(\pm 2.960)$	0.377
19	41	$M_S = 1.037(\pm 0.167) * m_b - 0.205(\pm 0.344)$	0.696
20	77	$M_S = 1.212(\pm 0.083) * m_b - 0.940(\pm 0.179)$	0.856
21	33	$M_S = 1.479(\pm 0.10) * m_b - 2.280(\pm 0.336)$	0.863
22	12	$M_S = 1.217(\pm 0.735) * m_b - 1.192(\pm 1.540)$	0.431
23	16	$M_S = 1.254(\pm 0.319) * m_b - 1.574(\pm 0.676)$	0.701
24	51	$M_S = 1.451(\pm 0.081) * m_b - 2.315(\pm 0.180)$	0.929
1	15	$M_S = 1.668(\pm 0.266) * M_D - 3.178(\pm 0.577)$	0.851
2	2	–	–
3	1	–	–
4	10	$M_S = 2.119(\pm 0.457) * M_D - 5.283(\pm 0.971)$	0.826
5	5	–	–
6	18	$M_S = 2.332(\pm 0.332) * M_D - 6.346(\pm 0.712)$	0.856
7	11	$M_S = 1.333(\pm 0.230) * M_D - 1.880(\pm 0.513)$	0.868
8	1	–	–
9	30	$M_S = 1.553(\pm 0.294) * M_D - 2.495(\pm 0.639)$	0.695
10	17	$M_S = 1.477(\pm 0.219) * M_D - 2.025(\pm 0.449)$	0.853
11	68	$M_S = 1.256(\pm 0.101) * M_D - 0.980(\pm 0.204)$	0.834
12	55	$M_S = 1.179(\pm 0.089) * M_D - 0.819(\pm 0.189)$	0.872
13	21	$M_S = 1.566(\pm 0.191) * M_D - 2.255(\pm 0.376)$	0.873
14	26	$M_S = 1.327(\pm 0.146) * M_D - 1.498(\pm 0.302)$	0.872
15	54	$M_S = 1.365(\pm 0.086) * M_D - 1.642(\pm 0.172)$	0.908
16	24	$M_S = 1.724(\pm 0.412) * M_D\ - 2.906(\pm 0.826)$	0.649
17	99	$M_S = 1.388(\pm 0.068) * M_D - 1.683(\pm 0.137)$	0.899
18	5	–	–
19	19	$M_S = 1.430(\pm 0.130) * M_D - 1.878(\pm 0.259)$	0.930
20	56	$M_S = 1.324(\pm 0.093) * M_D - 1.422(\pm 0.198)$	0.886
21	24	$M_S = 1.239(\pm 0.188) * M_D - 1.151(\pm 0.427)$	0.803
22	4	–	–
23	5	–	–
24	23	$M_S = 1.296(\pm 0.093) * M_D - 1.738(\pm 0.213)$	0.946
1	6	–	–
2	2	–	–
3	0	–	–
4	3	–	–
5	3	–	–
6	10	$M_S = 1.265(\pm 0.252) * M_L - 1.435(\pm 0.559)$	0.846
7	2	–	–
8	1	–	–
9	2	–	–
10	2	–	–
11	89	$M_S = 1.828(\pm 0.285) * M_L - 3.655(\pm 0.590)$	0.563
12	104	$M_S = 1.546(\pm 0.209) * M_L - 2.410(\pm 0.437)$	0.586
13	8	–	–
14	16	$M_S = 1.271(\pm 0.196) * M_L - 1.164(\pm 0.413)$	0.851
15	37	$M_S = 1.262(\pm 0.113) * M_L - 1.183(\pm 0.238)$	0.877
16	0	–	–
17	67	$M_S = 1.226(\pm 0.094) * M_L - 1.045(\pm 0.196)$	0.847
18	1	–	–
19	18	$M_S = 1.132(\pm 0.163) * M_L - 0.829(\pm 0.345)$	0.854
20	31	$M_S = 1.004(\pm 0.106) * M_L - 0.251(\pm 0.223)$	0.861
21	3	–	–
22	0	–	–
23	3	–	–
24	7	–	–
1	39	$m_b = 1.118(\pm 0.147) * M_D - 0.4484(\pm 0.309)$	0.772
2	20	$m_b = 1.208(\pm 0.195) * M_D - 0.671(\pm 0.399)$	0.811
3	25	$m_b = 1.054(\pm 0.215) * M_D - 0.004(\pm 0.445)$	0.700
4	24	$m_b = 1.272(\pm 0.184) * M_D - 1.123(\pm 0.391)$	0.815
5	5	–	–
6	34	$m_b = 1.436(\pm 0.251) * M_D - 1.996(\pm 0.534)$	0.700
7	36	$m_b = 0.929(\pm 0.097) * M_D + 0.204(\pm 0.212)$	0.848
8	3	–	–
9	70	$m_b = 1.057(\pm 0.064) * M_D - 0.079(\pm 0.135)$	0.891
10	60	$m_b = 0.925(\pm 0.103) * M_D + 0.423(\pm 0.211)$	0.756
11	134	$m_b = 1.293(\pm 0.082) * M_D - 0.939(\pm 0.165)$	0.806
12	123	$m_b = 1.081(\pm 0.093) * M_D - 1.285(\pm 0.192)$	0.722
13	18	$m_b = 0.747(\pm 0.264) * M_D + 1.235(\pm 0.524)$	0.554
14	32	$m_b = 0.939(\pm 0.107) * M_D + 0.317(\pm 0.221)$	0.841
15	38	$m_b = 1.076(\pm 0.124) * M_D - 0.242(\pm 0.263)$	0.815
16	62	$m_b = 0.914(\pm 0.105) * M_D + 0.487(\pm 0.215)$	0.742
17	79	$m_b = 1.155(\pm 0.122) * M_D - 0.617(\pm 0.252)$	0.729
18	11	$m_b = 1.086(\pm 0.083) * M_D - 0.398(\pm 0.167)$	0.970
19	21	$m_b = 1.363(\pm 0.195) * M_D - 1.432(\pm 0.396)$	0.836
20	57	$m_b = 0.948(\pm 0.059) * M_D + 0.200(\pm 0.129)$	0.904
21	139	$m_b = 0.889(\pm 0.057) * M_D + 0.464(\pm 0.120)$	0.796
22	14	$m_b = 0.737(\pm 0.199) * M_D + 1.028(\pm 0.416)$	0.702
23	15	$m_b = 2.045(\pm 0.534) * M_D - 4.605(\pm 1.102)$	0.703
24	52	$m_b = 0.906(\pm 0.084) * M_D + 0.374(\pm 0.182)$	0.831
1	13	$m_b = 0.621(\pm 0.102) * M_L + 1.804(\pm 0.216)$	0.861
2	10	$m_b = 1.258(\pm 0.261) * M_L - 0.977\ (\pm 0.550)$	0.836
3	1	–	–
4	12	$m_b = 0.494(\pm 0.101) * M_L + 2.303(\pm 0.211)$	0.816
5	4		–
6	17	$m_b = 0.752(\pm 0.143) * M_L + 1.112(\pm 0.312)$	0.788
7	2	–	–
8	1	–	–
9	13	$m_b = 0.985(\pm 0.217) * M_L + 0.277(\pm 0.442)$	0.783
10	11	$m_b = 0.791(\pm 0.109) * M_L + 0.949(\pm 0.233)$	0.909
11	199	$m_b = 1.135(\pm 0.099) * M_L - 0.418(\pm 0.205)$	0.630
12	249	$m_b = 1.661(\pm 0.144) * M_L - 2.647(\pm 0.297)$	0.590
13	15	$m_b = 2.162(\pm 0.648) * M_L - 4.943(\pm 1.345)$	0.653
14	43	$m_b = 1.044\ (\pm 0.159) * M_L + 0.056(\pm 0.321)$	0.707
15	125	$m_b = 0.961(\pm 0.062) * M_L + 0.189(\pm 0.126)$	0.809
16	5	–	–
17	220	$m_b = 0.932(\pm 0.048) * M_L +\ 0.376(\pm 0.096)$	0.792
18	3	–	–
19	38	$m_b = 0.899(\pm 0.110) * M_L + 0.243(\pm 0.227)$	0.798
20	42	$m_b = 0.872(\pm 0.127) * M_L + 0.450(\pm 0.265)$	0.728
21	11	$m_b = 0.985(\pm 0.196) * M_L + 0.090(\pm 0.406)$	0.835
22	4	–	–
23	11	$m_b = 1.947(\pm 0.933) * M_L - 3.812(\pm 1.892)$	0.532
24	17	$m_b = 0.706(\pm 0.062) * M_L + 1.427(\pm 0.140)$	0.939
1	20	$M_D = 0.881(\pm 0.138) * M_L + 0.596(\pm 0.286)$	0.820
2	14	$M_D = 0.919(\pm 0.023) * M_L + 0.292(\pm 0.048)$	0.996
3	11	$M_D = 0.991(\pm 0.080) * M_L + 0.033(\pm 0.158)$	0.966
4	24	$M_D = 0.768(\pm 0.114) * M_L + 1.004(\pm 0.239)$	0.808
5	4	–	–
6	26	$M_D = 0.816(\pm 0.068) * M_L + 0.825(\pm 0.147)$	0.920
7	14	$M_D = 0.812(\pm 0.112) * M_L + 0.726(\pm 0.234)$	0.889
8	2	–	–
9	11	$M_D = 0.432(\pm 0.339) * M_L + 2.293(\pm 0.675)$	0.359
10	23	$M_D = 0.843(\pm 0.066) * M_L + 0.580(\pm 0.137)$	0.935
11	81	$M_D = 0.818(\pm 0.036) * M_L + 0.586(\pm 0.075)$	0.929
12	46	$M_D = 1.277(\pm 0.209) * M_L - 1.372(\pm 0.434)$	0.669
13	12	$M_D = 1.113(\pm 0.389) * M_L - 0.555(\pm 0.768)$	0.636
14	29	$M_D = 0.956(\pm 0.057) * M_L + 0.103(\pm 0.114)$	0.952
15	70	$M_D = 0.934(\pm 0.029) * M_L + 0.163(\pm 0.062)$	0.967
16	15	$M_D = 0.446(\pm 0.146) * M_L + 1.900(\pm 0.291)$	0.619
17	67	$M_D = 0.748(\pm 0.043) * M_L + 0.869(\pm 0.089)$	0.903
18	12	$M_D = 0.886(\pm 0.044) * M_L + 0.349(\pm 0.087)$	0.985
19	18	$M_D = 0.901(\pm 0.049) * M_L + 0.268(\pm 0.100)$	0.974
20	62	$M_D = 0.939(\pm 0.068) * M_L + 0.091(\pm 0.138)$	0.867
21	22	$M_D = 0.876(\pm 0.069) * M_L + 0.450(\pm 0.139)$	0.939
22	17	$M_D = 0.873(\pm 0.043) * M_L + 0.467(\pm 0.089)$	0.980
23	11	$M_D = 1.229(\pm 0.691) * M_L - 0.707(\pm 1.382)$	0.473
24	21	$M_D = 0.743(\pm 0.099) * M_L + 1.211(\pm 0.222)$	0.851

The relationships are calculated by the orthogonal regression method. The values in the parentheses show the uncertainties. These functional relations were used to construct a homogeneous catalogue.

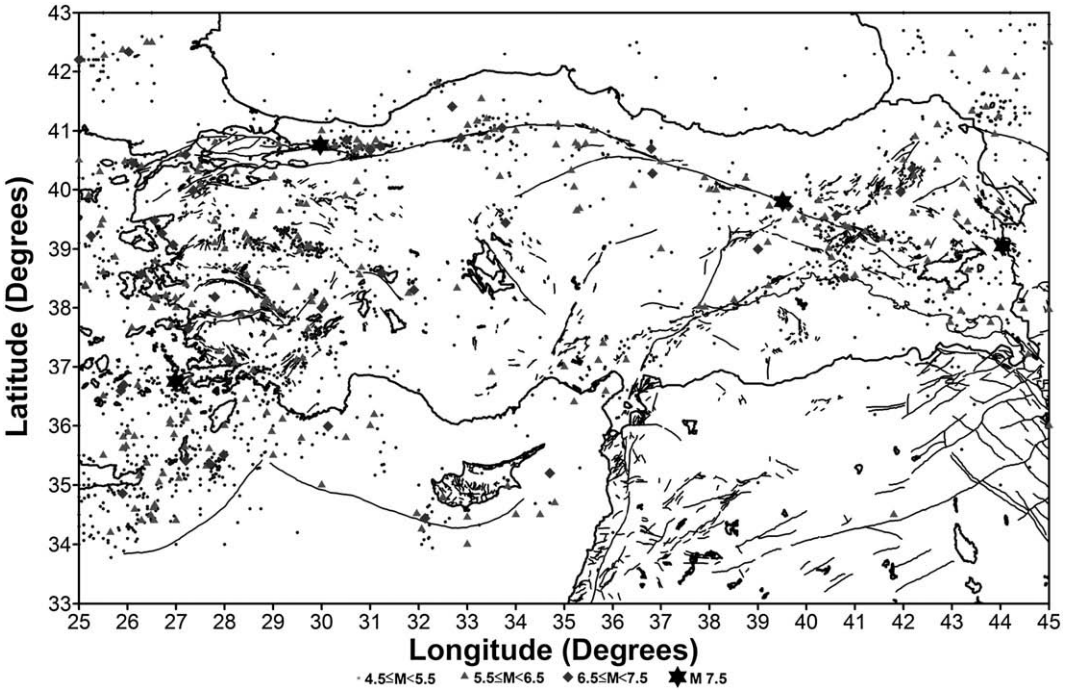

Fig. 3. Epicenter locations of earthquakes in Turkey from 1900 to 2005 with major tectonic features. Magnitude size of earthquakes are shown by different symbol.

$M_S = 7.8$. The Erzincan and İzmit earthquakes are related to the NAFZ, but the Rhodes and Van earthquakes are related to the Aegean arc and KITÇF, respectively. Other large earthquakes between 7.0 and 7.5 are observed in the Aegean region and NAFZ, but large earthquakes are not observed in the BTZ and EAFZ. All earthquakes with maximum observed magnitudes $M_{\max}^{\text{obs}}$, locations and dates are given in Table 2. The smallest earthquakes in the catalog are: 1995 Cyprus Region, $M_S = 5.2$ and 1915 Şanlıurfa, $M_S = 5.4$. The number of earthquakes in these regions is also quite small, fewer than 20 events. The region with the maximum number of events is region 17, where 24785 earthquakes have been located. High seismicity levels are also observed in regions 11, 14, 16, 19, 20 and 21, related to the Aegean Region and NAFZ. The observed seismicity in the regions including the NAFZ is lower than that of the Aegean Region.

In seismicity studies, it is frequently necessary to use the maximum number of events available for high-quality results. It known that magnitude completeness changes with time in most catalogs and usually decreases. The minimum completeness is therefore an important parameter for seismicity studies. The catalog used in the study was constructed for all time periods and the different 24 seismic source zones as shown in Table 3. The method used to assess the completeness of the data of this catalog has been described elsewhere (e.g., Tsapanos, 1990; Tsapanos and Papazachos, 1998). The completeness was assessed on the basis of the cumulative frequency distribution of the magnitudes, and of the cumulative frequency distribution of the number of earthquakes with magnitudes larger than a certain value. Thus, the final catalog encompasses the time period from 1900 to 2005, and this is the instrumental part of the catalog.

4. Method for estimating the earthquake hazard parameters

The maximum regional magnitude earthquake, $\hat{M}_{\max}$, is defined here as the upper limit of the magnitude for the given seismic tectonic source (Reiter, 1990). The procedure for evaluating the maximum regional magnitude $\hat{M}_{\max}$ is based on the equation that compares the largest *observed* magnitude $M_{\max}^{\text{obs}}$ and the maximum *expected* magnitude $E(\hat{M}_{\max}/T)$ during the span, T, of the catalog (Kijko, 1988, 2004). If this condition is applied to the Gutenberg–Richter frequency–magnitude distribution, the following estimator of maximum regional magnitude $\hat{M}_{\max}$ is obtained (Kijko, 1988):

$$\hat{M}_{\max} = M_{\max}^{\text{obs}} + \frac{E_1(TZ_2) - E_1(TZ_1)}{\hat{\beta}\exp(-TZ_2)} + M_{\min}\exp\left(-\hat{\lambda}T\right) \quad (1)$$

The above estimator of $\hat{M}_{\max}$ for the doubly-truncated Gutenberg–Richter relation was first obtained by Kijko (1983). The quantities

Table 2
Different 24 seismic regions in and around Turkey, the number of earthquakes, observed maximum magnitudes in each region and their date and locations.

Region	Number of earthquakes	$M_{\max}^{\text{obs}}$ (observed maximum magnitude)	Date (m.d.y)	Location	Data source
1	945	6.8	09.13.1924	Pasinler	KOERI
		6.8	10.30.1983	Horasan	
2	129	7.5	11.24.1976	Çaldıran–Muradiye	KOERI
3	101	6.3	04.28.1903	Patnos	ISC
4	596	6.6	09.06.1975	Lice–Diyarbakır	KOERI
5	20	5.4	05.19.1915	Şanlıurfa	KOERI
6	600	5.9	08.11.2004	Elazığ	KOERI
7	688	6.0	02.17.1908	Adana–Ceyhan	KOERI
		6.0	03.20.1945	Adana–Ceyhan	
8	11	5.2	02.14.1995	Cyprus Region	KOERI
9	482	6.7	10.091996	Cyprus Region	KOERI
10	1074	6.8	03.18.1926	Finike	ISC
11	4508	7.7	06.26.1926	Rhodes	ISC
12	1711	7.4	07.09.1956	Aegean Sea	ISC
13	1504	6.4	03.01.1926	Burdur	KOERI
14	3173	6.8	07.16.1955	Aydın–Söke	KOERI
15	5368	6.6	07.23.1949	İzmir–Karaburun	KOERI
16	3155	7.0	04.09.1931	Akşehir	KOERI
17	24785	7.2	12.19.1981	Aegean Sea	ISC
18	697	6.4	02.20.1956	Eskişehir	ISC
19	5781	7.2	03.18.1953	Çanakkale–Yenice	KOERI
20	9292	7.8	08.17.1999	İzmit	KOERI
21	3715	7.4	11.12.1999	Düzce	KOERI
22	103	6.6	04.19.1938	Kırsehir	ISC
23	87	6.8	12.04.1905	Çemişgezek	ISC
24	2042	7.9	12.26.1939	Erzincan	KOERI

Table 3
Magnitude completeness for instrumental period in 24 different source regions of Turkey.

Region	Period of years	Magnitude threshold
1	1906	$M_S \geq 5.5$
	1949	$M_S \geq 5.0$
	1975	$M_S \geq 3.5$
2	1941	$M_S \geq 5.5$
	1977	$M_S \geq 4.0$
3	1903	$M_S \geq 6.0$
	1930	$M_S \geq 5.0$
	1966	$M_S \geq 4.0$
	1982	$M_S \geq 3.5$
4	1908	$M_S \geq 5.5$
	1965	$M_S \geq 5.0$
	1975	$M_S \geq 4.0$
	1995	$M_S \geq 3.0$
	2004	$M_S \geq 1.0$
5	1915	$M_S \geq 5.4$
	1936	$M_S \geq 5.0$
	1965	$M_S \geq 4.5$
	1978	$M_S \geq 4.1$
6	1949	$M_S \geq 5.0$
	1971	$M_S \geq 4.5$
	1986	$M_S \geq 3.5$
	1995	$M_S \geq 3.0$
	2002	$M_S \geq 1.0$
7	1908	$M_S \geq 5.5$
	1951	$M_S \geq 5.0$
	1988	$M_S \geq 4.0$
	1998	$M_S \geq 2.0$
8	1980	$M_S \geq 3.5$
	1988	$M_S \geq 3.0$
9	1918	$M_S \geq 6.0$
	1953	$M_S \geq 5.5$
	1993	$M_S \geq 5.0$
	1996	$M_S \geq 3.0$
10	1926	$M_S \geq 5.0$
	1958	$M_S \geq 4.5$
	1979	$M_S \geq 4.0$
	1983	$M_S \geq 3.5$
	1987	$M_S \geq 3.0$
	1994	$M_S \geq 2.5$
11	1918	$M_S \geq 5.5$
	1970	$M_S \geq 4.5$
	1990	$M_S \geq 3.5$
12	1910	$M_S \geq 5.5$
	1956	$M_S \geq 5.0$
	1973	$M_S \geq 4.0$
13	1926	$M_S \geq 5.5$
	1971	$M_S \geq 4.5$
	1991	$M_S \geq 3.0$
	1996	$M_S \geq 2.3$
14	1904	$M_S \geq 6.0$
	1928	$M_S \geq 5.0$
	1954	$M_S \geq 4.0$
	1984	$M_S \geq 3.0$
15	1904	$M_S \geq 5.5$
	1933	$M_S \geq 5.0$
	1965	$M_S \geq 4.0$
	1975	$M_S \geq 3.0$
16	1914	$M_S \geq 5.0$
	1970	$M_S \geq 4.5$
	1993	$M_S \geq 4.0$
	2002	$M_S \geq 2.1$
17	1903	$M_S \geq 5.5$
	1920	$M_S \geq 5.0$
	1970	$M_S \geq 4.5$
	1986	$M_S \geq 2.5$
	1998	$M_S \geq 2.1$
18	1926	$M_S \geq 5.0$
	1961	$M_S \geq 4.5$
	1977	$M_S \geq 3.8$
19	1905	$M_S \geq 5.5$
	1953	$M_S \geq 4.5$
	1983	$M_S \geq 2.5$
	1989	$M_S \geq 2.0$
20	1907	$M_S \geq 5.0$
	1951	$M_S \geq 4.5$
	1975	$M_S \geq 3.5$
	1990	$M_S \geq 2.2$
21	1904	$M_S \geq 5.5$
	1944	$M_S \geq 5.0$
	1967	$M_S \geq 4.0$
	1998	$M_S \geq 2.2$
22	1921	$M_S \geq 5.5$
	1941	$M_S \geq 5.0$
	1960	$M_S \geq 4.5$
	1972	$M_S \geq 4.0$
	1985	$M_S \geq 3.6$
23	1905	$M_S \geq 5.5$
	1922	$M_S \geq 5.0$
	1971	$M_S \geq 4.0$
	1986	$M_S \geq 3.4$
24	1929	$M_S \geq 5.0$
	1971	$M_S \geq 4.0$
	2002	$M_S \geq 2.2$

in Eq. (1) are computed as: $Z_1 = \hat{\lambda} A_1 / (A_1 - A_2)$, $Z_2 = \hat{\lambda} A_2 / (A_1 - A_2)$, $A_1 = \exp(-\hat{\beta} M_{\min})$, and $A_2 = \exp(-\hat{\beta} M_{\max}^{obs})$, and $E_1(.)$ denotes an exponential integral function (Abramowitz and Stegum, 1970):

$$E_1(z) = \int_z^{\infty} exp(-\zeta) / \zeta d\zeta \tag{2}$$

It is not difficult to show that the approximate variance of the maximum regional magnitude $\hat{M}_{\max}$, estimated according to Eq. (1), is equal to that derived by Kijko (2004):

$$\mathrm{Var}\left(\hat{M}_{\max}\right) = \hat{\sigma}_M^2 + \left[\frac{E_1(TZ_2) - E_1(TZ_1)}{\hat{\beta}\exp(-TZ_2)} + M_{\min}\exp\left(-\hat{\lambda}T\right)\right]^2 \tag{3}$$

where it is assumed that the observed (apparent) magnitude is distorted by an observational error, which is distributed normally with a known standard deviation $\hat{\sigma}_M$ (Kijko and Dessokey, 1987).

The parameters $\hat{\beta}$ and $\hat{\lambda}$ for a given area are estimated by the maximum likelihood procedure described by Kijko and Sellevoll (1989, 1992). This method allows for all available seismicity information to be used, as it makes use of an earthquake catalog containing both incomplete historical observations and more congruous and complete instrumental data. Periods with gaps in the catalog can also be taken into account. Eq. (1) is applicable even in cases where the considered magnitude interval, $M_{\max} - M_{\min}$, is short and the number of events small.

5. Results

All the examined regions belong to Turkey and the nearby areas. The tectonics of the area are described above. The values of the maximum regional magnitude $\hat{M}_{\max}$, the parameter $\hat{b}$ of the Gutenberg–Richter relationship and the mean activity rate $\hat{\lambda}$, estimated for the 24 regions, are shown in Table 4.

Two are the main tectonic features in Turkey are 1) the NAFZ (regions 19, 20, 21, 24) and 2) the EAFZ (regions 3, 4, 5, 6). Due to the different adopted cutoffs, it is not possible to compare the $\hat{\lambda}$ obtained for the aforementioned regions. However, just for academic reasons, we point out that the NAFZ has a mean activity rate of $\hat{\lambda} = 62.90$, which is not very different from the corresponding one of the EAFZ of $\hat{\lambda} = 63.89$. The mean activity rate in the examined area varies between 0.16 (in region 8) and 238 (in region 16).

The obtained parameter $\hat{b}$ shows totally different values between the NAFZ and the EAFZ, with average values of 0.999 and 0.714,

Table 4
The values of earthquake hazard parameters for 24 seismic regions: a) the $\hat{b}$ value and its standard deviation; b) the mean seismic activity rate $\hat{\lambda}$ and its standard deviation; c) the minimum magnitude for the regions; d) the maximum regional magnitude $\hat{M}_{max}$ and its standard deviation; d) the return period (RP) of earthquake magnitude $M \geq 6.0$ and, e) the index K.

Region	$\hat{b}$	$\sigma\hat{b}$	$\hat{\lambda}$	$\sigma\hat{\lambda}$	M_{min}	$\hat{M}_{max}$	$\sigma\hat{M}_{max}$	M_{max}^{obs}	$RP_{6.0}$	K
1	0.76	0.04	3.50	0.35	3.4	7.20	0.45	6.8	33.4	5
2	0.86	0.05	1.33	0.22	3.9	7.50	0.25	7.5	45.7	6
3	0.60	0.04	2.26	0.30	2.9	6.57	0.37	6.3	62.8	3
4	0.61	0.01	146.86	8.80	0.9	6.65	0.21	6.6	17.1	4
5	1.00	0.04	0.44	0.12	4.0	5.66	0.33	5.4	–	–
6	0.64	0.02	106.02	5.41	1.0	5.97	0.21	5.9	–	–
7	0.79	0.02	63.75	3.08	1.9	6.07	0.21	6.0	261.8	2
8	0.89	0.07	0.16	0.07	2.9	5.70	0.54	5.2	–	–
9	0.86	0.03	32.70	1.90	2.9	6.84	0.24	6.7	19.8	5
10	0.76	0.02	38.13	1.51	2.4	6.96	0.30	6.8	19.8	5
11	1.15	0.03	33.47	1.47	3.4	8.20	0.54	7.7	35.5.	6
12	1.10	0.03	15.27	0.75	3.9	7.90	0.58	7.4	15.4	6
13	0.82	0.02	62.75	2.65	2.2	6.51	0.23	6.4	39.5	4
14	1.09	0.03	34.02	1.37	2.9	7.29	0.55	6.8	88.4	4
15	1.13	0.02	39.71	1.01	3.1	6.84	0.38	6.6	62.5	4
16	1.11	0.02	238.26	8.72	2.2	7.36	0.41	7.0	92.7	4
17	1.02	0.02	76.71	2.20	2.9	7.46	0.40	7.2	22.9	5
18	0.85	0.05	1.09	0.18	3.7	6.90	0.58	6.4	110.3	3
19	0.97	0.02	63.57	1.86	2.4	7.55	0.46	7.2	59.2	5
20	1.07	0.02	93.12	2.64	2.6	8.30	0.58	7.8	58.1	5
21	1.02	0.02	69.87	3.08	2.9	7.81	0.51	7.4	25.0	6
22	0.94	0.04	2.07	0.29	3.5	7.10	0.54	6.6	131.4	3
23	0.87	0.04	2.13	0.31	3.3	7.30	0.64	6.8	130.2	3
24	0.93	0.03	25.06	2.27	2.9	8.10	0.54	7.9	75.2	5

The maximum observed magnitude for comparison purposes is also given for each region.

respectively. In order to avoid bias estimation, the t-test was applied to both populations of the NAFZ and the EAFZ. The results show that the parameter t (of the t-test) equals 2.805, which corresponds to a probability of 3% that the two groups of $\hat{b}$ values (belonging to the NAFZ and EAFZ) have the same mean. The probability is very low, and hence we can conclude that the two groups have different means.

On the regional scale, the estimated $\hat{M}_{max}$ values do not differ from the observed. Their differences vary between 0.00 (region 2) and 0.50 in 7 regions (8, 11, 12, 18, 19, 22 and 23). The largest values of $\hat{M}_{max} \geq 7.8$ are found in regions 11, 12, 20, 21 and 24. We note that regions 11 and 12 belong to the Aegean arc, which is a very seismically active area, where earthquakes of magnitude ~8 have occurred in the historical era (365 A.D. $M = 8.3$ Crete island, 1926 $M = 7.7$ Rhoades island) due to the underthrusting of Africa under the Eurasian plate. The other three regions, 20, 21 and 24, are parts of the very dangerous NAFZ (1939 $M = 7.9$ Erzincan, 1999 $M = 7.8$ İzmit).

Beyond those individual regions, almost all of the examined regions are characterized by medium to high levels of seismicity. All of them have frequently experienced large earthquakes ($M \geq 6.0$) that caused damages and/or fatalities. As shown in Table 4, the return periods (RP) of earthquakes with $M \geq 6.0$ are important, because this magnitude is considered to be dangerous, and the values of RP are reliable for further processing. In order to classify the examined regions in groups based on their hazard level, we applied the technique of Tsapanos (2001). Along with this technique, the $\hat{M}_{max}$ and $RP_{6.0}$ for each region are also taken into account. We considered that the seismic hazard is a function of the form $\Theta(\hat{M}_{max}, RP_{6.0})$, increasing with $\hat{M}_{max}$ and decreasing with $RP_{6.0}$. In this way, the following groups were reconstructed: $6.00 \leq \hat{M}_{max} \leq 6.80$, $6.81 \leq \hat{M}_{max} \leq 7.49$ and $\hat{M}_{max} \geq 7.50$, and we defined $\Theta(\hat{M}_{max})$ to be equal to 2, 4 and 6, respectively. Similarly, $\Theta(RP_{6.0})$ is defined equal to 6, 4 and 2 for the corresponding $RP_{6.0} \leq 50$, $51 \leq RP_{6.0} \leq 100$ and $RP_{6.0} \geq 101$. The arithmetic mean $K = \frac{1}{2}[\Theta(M_{max}) + \Theta(RP_{6.0})]$ signifies the adopted relative earthquake hazard level of a specific region. The index K takes values of 2, 3, 4, 5 and 6. Based on the above five groups, the relative earthquake hazards are defined as: very low, low, intermediate, high and very high, respectively. Admittedly, a number of exceptions exist: in regions 5, 6 and 8, neither $\hat{M}_{max}$ nor M_{max}^{obs} exceed a magnitude of 6.0. In Fig. 6, the index K is plotted for the 24 regions. Five groups are formed given the exceptions that exist for regions 5, 6 and 8.

6. Discussion and conclusions

We try to evaluate the seismicity and earthquake hazard parameters of Turkey. For this purpose, we divided Turkey into 24 seismic regions and used data including the instrumental period between 1900 and 2005. The maximum regional magnitude $\hat{M}_{max}$, the parameter $\hat{b}$ of the Gutenberg–Richter relationship and the mean seismic activity rate $\hat{\lambda}$ are estimated using the maximum likelihood method for all of the areas referred to above. In order to estimate the maximum earthquake magnitude, $\hat{M}_{max}$, for specific seismotectonic sources, we applied Eq. (1) (Kijko, 1988, 2004), whereas the other parameters ($\hat{b}$ and $\hat{\lambda}$) are computed by the method proposed by Kijko and Sellevoll (1989, 1992). The values of the earthquake hazard parameters and their standard deviations for the different 24 seismic regions of Turkey are listed in Table 4. The maximum observed earthquake magnitudes M_{max}^{obs} are also given in Table 4.

The estimated $\hat{M}_{max}$ values are between 5.66 and 8.30. These values were distributed into three groups, 5.60–6.80, 6.81–7.50 and greater than 7.50. The three groups of $\hat{M}_{max}$ values are shown with different grey scales, as shown in Fig. 4. The values greater than 7.50 are found in regions 11, 12, 19, 20, 21 and 24. The largest $\hat{M}_{max}$ value appears in the Marmara part of the NAFZ (İzmit, region 20 with $\hat{M}_{max} = 8.30$), where the largest earthquake recently occurred in 1999, with a maximum observed magnitude $M_{max}^{obs} = 7.80$. The other largest values of $\hat{M}_{max}$ are calculated near Rhodes (region 11 with $\hat{M}_{max} = 8.20$), where the largest event occurred in 1926 with $M_{max}^{obs} = 7.70$, and in Erzincan (region 24 with $\hat{M}_{max} = 8.10$), where the largest earthquake of the present century occurred in 1939 with a maximum observed magnitude of $M_{max}^{obs} = 7.90$, in the Aegean arc (region 12 with $\hat{M}_{max} = 7.90$), where the largest earthquakes occurred in 1956 with $M_{max}^{obs} = 7.40$; in the Anatolian part of the NAFZ (Düzce, region 21 with $\hat{M}_{max} = 7.81$) in which the events occurred in 1999 with $M_{max}^{obs} = 7.40$, and in the Yenice–Gönen Fault Zone (Çanakkale, region 19 with $\hat{M}_{max} = 7.55$) where the largest earthquake occurred in 1953 with $M_{max}^{obs} = 7.20$. These regions where the largest $\hat{M}_{max}$ values are observed are related to the NAF and the Aegean arc. Intermediate $\hat{M}_{max}$ values between 6.81 and 7.50 are found in regions 1, 2, 9, 10, 14, 15, 16, 17, 18, 22 and 23. The M_{max}^{obs} of earthquakes that occurred in these regions are between 6.40 and 7.50, as listed in Tables 3 and 4. These $\hat{M}_{max}$ values are related to the graben and faults in the Aegean region and NEAFZ. Although regions 22 and 23 are characterized by low seismicity, as shown in Figs. 2 and 3 and Table 2, their $\hat{M}_{max}$ values are computed to be 7.10 and 7.30, respectively. These high values depend on the 1938 Kırşehir ($M = 6.60$) and 1905 Çemişgezek ($M = 6.80$) earthquakes. There is no clear evidence for a pattern between $\hat{M}_{max}$ and M_{max}^{obs} values, although these parameters are closer to each other in some regions. In regions 14, 18, 22, and 23 there are about 0.5 unit differences between these two parameters, but there is no/less difference in the other regions. Values of $\hat{M}_{max}$ lower than 6.80 are calculated in regions 3, 4, 5, 6, 7, 8, and 13, which include the BTZ, the EAFZ, part of the Dead Sea fault, the northern part of Cyprus and the BFZ. In these regions, the M_{max}^{obs} change to 5.20 and 6.60, as given in Tables 3 and 4. There is a 0.5 unit difference between M_{max}^{obs} and $\hat{M}_{max}$ values in region 8, whereas the values in other regions are similar. We note that the fault systems in the regions where the $\hat{M}_{max}$ are greater than the M_{max}^{obs} have a capacity to generate larger earthquakes than the observed shocks. As stated above, only instrumental datasets were examined. The maximum observed magnitude for each region is extracted from these datasets. However, in some regions we have historical data with maximum magnitudes that exceed to various degrees the maximum observed magnitudes from the instrumental period. For example, in region 1 the maximum magnitude ever observed occurred in 1458 with a $M_{max}^{hist} = 7.5$. The applied method verifies in some ways the reliability of

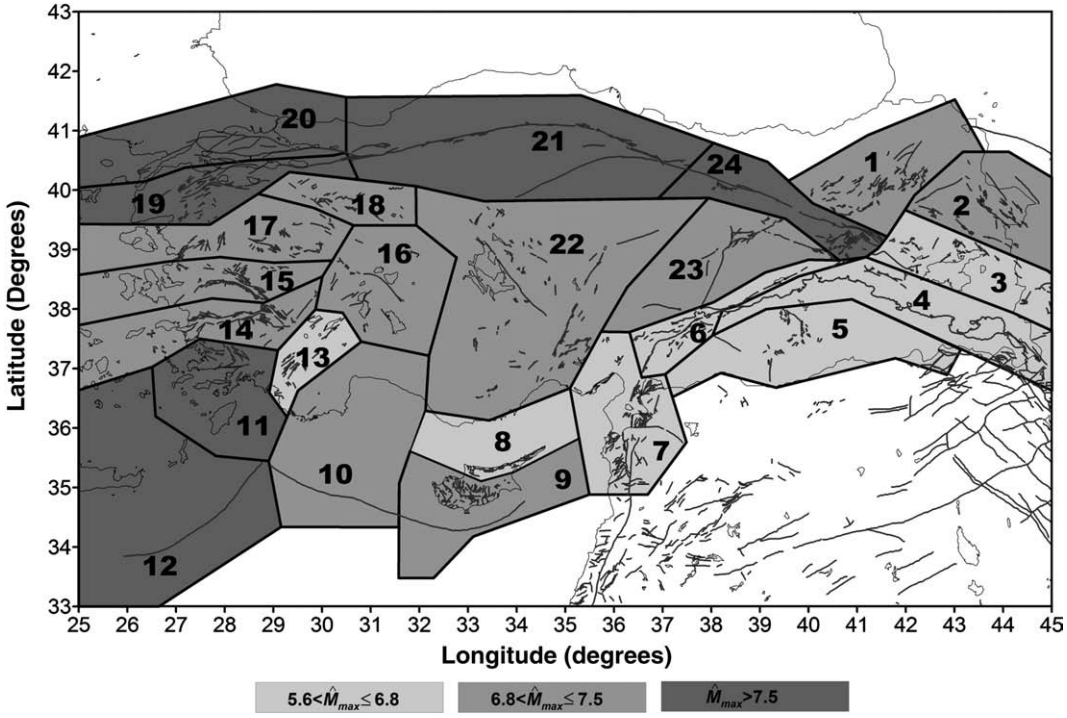

Fig. 4. $\hat{M}_{max}$ values for different 24 seismic source regions in and around Turkey.

our results. The estimated $\hat{M}_{max} = 7.20$ is much closer to the magnitude of the historical era, instead of the magnitude $M_{max}^{obs} = 6.8$ observed in the instrumental period. Moreover, if we add $\hat{M}_{max} + \sigma\hat{M}_{max} = 7.65$, the output result is very similar to the M_{max}^{hist}. The computed uncertainties are therefore very promising regarding the comparison between the $\hat{M}_{max}$ and the M_{max}^{hist}.

The computed $\hat{b}$ values vary between 0.60 and 1.15. The $\hat{b}$ values were distributed into three groups: 0.60–0.80, 0.81–1.00 and larger than 1.00. The three groups drawn in grey scale are shown in Fig. 5. The $\hat{b}$ values larger than 1.00 are found in regions 11, 12, 14, 15, 16, 17, 20, and 21. Region 11, where the highest value is found at 1.15 in this group, and region 12, are related to the Aegean arc. Regions 14, 15, 16 and 17 are covered by grabens and faults in the Aegean region. However, regions 20 and 21 are related to the Marmara and Anatolian parts of the NAFZ, respectively. The second-level $\hat{b}$ values vary between 0.81 and 1.00 and are found in regions 2, 5, 8, 9, 13, 18, 19, 22, 23 and 24. The KITÇF, KEZ, Cyprus arc, BFZ, EİDKF, YGMUEF, MAFS, OMF, and ENAFZ cover these regions. The lowest $\hat{b}$ values varying

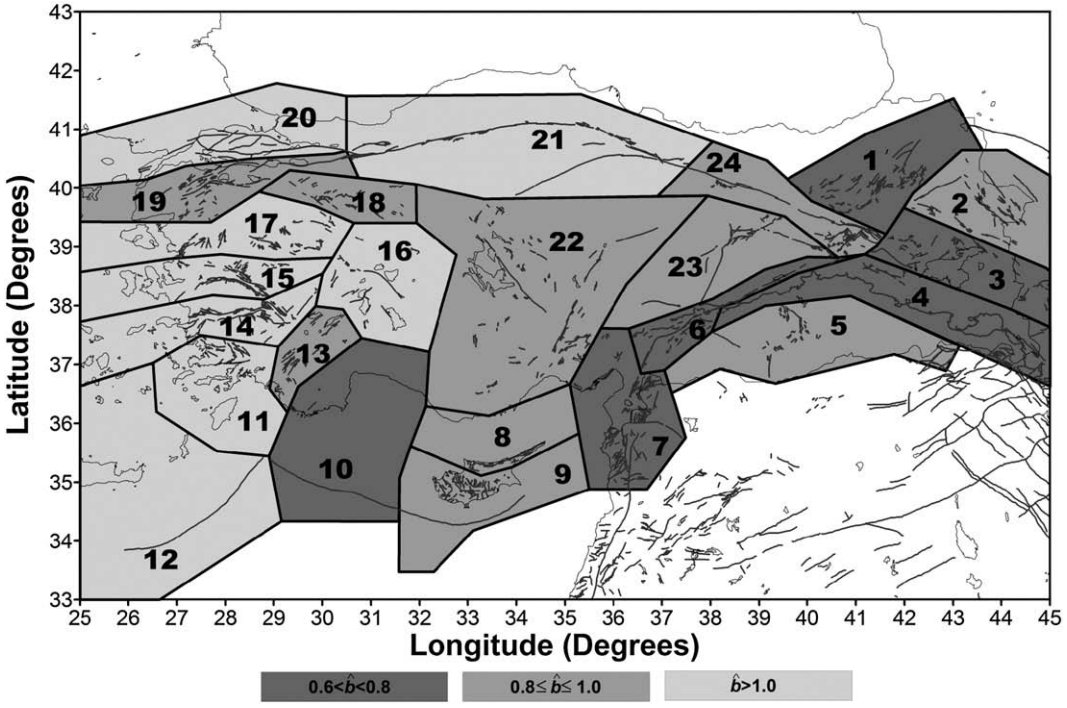

Fig. 5. $\hat{b}$ values for different 24 seismic source regions in and around Turkey.

between 0.60 and 0.80 in the third group are found in regions 1, 3, 4, 6, 7, and 10. These regions are related to the NEAFZ, MESF, BTZ, EAFZ, part of the Dead Sea fault and the western part of the Cyprus arc. In general, there is linear relation between $\hat{b}$ and $\hat{M}_{max}$, as seen in Table 4 and Figs. 5 and 6. For example, $\hat{M}_{max}$ values greater than 7.50 and $\hat{b}$ values greater than 0.93 are found in regions 11, 12, 19, 20, 21 and 24, while the lowest values of both parameters are found in regions 3, 4, 6, 7 and 10. However, regions 5 and 8 diverge from this linear trend. Since seismic activity is very low in these regions, as seen in Table 2, this divergence may depend on the number of observed earthquakes. Scholz (1968) stated that low $\hat{b}$ values mean large stress and strain in a given region. This can be interpreted as the region being promising for an earthquake generation. Thus, we can expect large earthquakes in regions 1, 3, 4, 6, 7, and 10 related to the NEAFZ, MESF, BTZ, EAFZ, part of the Dead Sea fault and the western part of the Cyprus arc. Region 10, which is situated between two active regions of the Aegean and Cyprus, where both experience large earthquakes, is particularly likely. This region seems to not have broken for a long time, since 1926. Regions 3 (unbroken since 1903) and 4 (unbroken since 1975), which are parts of the aseismic EAFZ, are also likely. However, the part between Erzincan and Erzurum in region 1 and part of the Dead Sea fault in region 7 have not broken and generated large earthquakes in the instrumental period.

The mean activity rate $\hat{\lambda}$ varies from 0.16 to 238.26. The lowest $\hat{\lambda}$ values, between 0 and 3.5, are found in regions 8, 5, 18, 2, 22, 23, 3, and 1, while the largest ones, greater than 100.0, are computed in regions 16, 4, and 6. The other values, varying from 15.27 to 93.12, are calculated in regions 12, 24, 9, 11, 14, 10, 15, 13, 19, 7, 21, 17, and 20. The largest $\hat{\lambda}$ value is 238.26 and is calculated in the SBTF (region 16). The other larger values are 146.86 on the BTZ (region 4) and 106.02 around the EAFZ (region 6). One interesting observation is that the mean activity rate in regions 16, 4, and 6 is rather large relative to other regions, while the values in regions 8, 5, 18, 2, 22, 23, 3, and 1 are rather small. When we compare the number of earthquakes in these regions to the number in other regions, it can be seen that the number of events above a certain magnitude per year in these regions (smaller $\hat{\lambda}$) is smaller than in the other regions (larger $\hat{\lambda}$). This means that in a given time interval, the number of earthquakes expected to occur in the smaller $\hat{\lambda}$ region is lower than the expected number of earthquakes in the same time interval in a region where the $\hat{\lambda}$ value is larger.

The uncertainties assessed for $\hat{b}$ values are negligible and cannot really affect the results. The mean activity rate $\hat{\lambda}$ reveals low uncertainties, none of them exceeding the values of $\hat{\lambda}$. This is due to the good quality of the data.

We provide a map based on the different earthquake hazard levels of the examined regions; this is an essential part of this work. The earthquake hazard levels were computed by considering that this parameter increases with $\hat{M}_{max}$ and decreases with RP as a function of the form $\Theta(\hat{M}_{max}, RP_{6.0})$. As relative earthquake hazard scale is defined as the index K and is calculated regionally. The values of the index K are: 2, 3, 4, 5 and 6, which is the largest. According to this, we classified the regions in the 5 groups as very low, low, intermediate, high and very high earthquake hazard levels. A first inspection in Fig. 6 reveals something interesting. If we look at the NAFZ, we find that regions 20 and 24 show high seismicity, because in these regions the large earthquakes of Erzincan and İzmit occurred. The middle part of the NAFZ between Bolu and Erzincan (particularly region 21) shows a very high level, because it is unbroken by very large earthquakes ($M \geq 7.8$, like those in Erzincan and İzmit), and the largest earthquake in this part occurred in 1943 (Tosya–Ladik earthquake), with $M = 7.2$. Other parts with very high seismicity in the examined area are regions 11 and 12, which are closely related to the Aegean arc/subduction. Region 2 also shows a very high level, which may be related to the large earthquake of 1976 Çaldıran–Muradiye ($M_S = 7.5$). The regions with high seismicity are 1, 9, 10, 17, 19, 20 and 24. An intermediate level dominates mainly in Minor Asia and the east Aegean Sea, while region 4 is of same level and it is just on the opposite side. A large zone of low seismicity occupies central Turkey and extends further into region 3. The only region with a very low level is region 7. In this study, the K index is calculated for $\hat{M}_{max}$ values that exceed 6.0.

Since the $\hat{M}_{max}$ values in regions of 5, 6 and 8 are smaller than 6.0, we cannot compute K values for these regions (see Table 4). We therefore

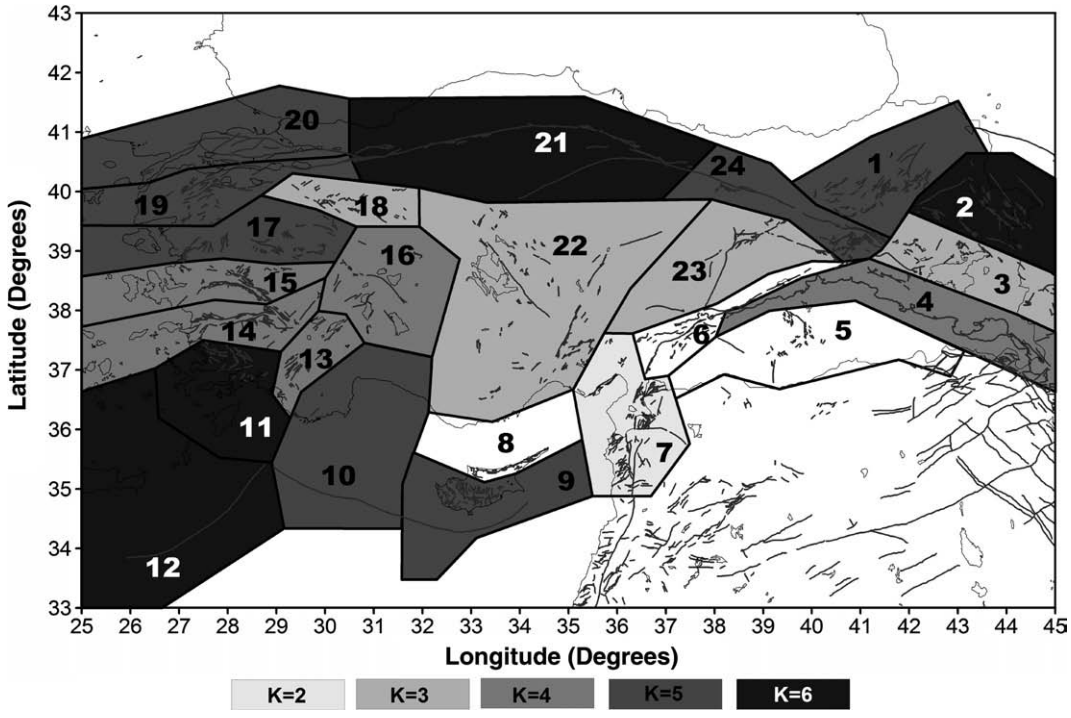

Fig. 6. K (relative hazard level) values for different 24 seismic source regions in and around Turkey.

did not mention these zones of low seismicity. The distribution of hazard level from region to region is informative and useful from a practical point of view. The relative hazard classification could be useful for engineers, planners, or for other scientific purposes, allowing the designation of priority regions for earthquake resistant designs.

Acknowledgements

The authors would like to express their sincere thanks to Dr. A. Kijko for the suggestions made in order for the paper to be improved. S. Öztürk is grateful to Karadeniz Technical University (Turkey) for partially supporting this work (project number: 2006.112.007.2). Also, G. Koravos, is grateful to GSRT (Greece) for partially supported this work by the project EPAN-M.4.3.6.1B. Also, the authors thank to Dr. C. Walker from Napier University in U.K. for editing the paper about English.

During the review of the paper we lost our beloved colleague George Leventakis. The present paper is dedicated to his memory.

References

Abramowitz, M., Stegum, I.R., 1970. Handbook of Mathematical Functions, 9th edition. Dover Publ., New York, p. 1046.
Alptekin, Ö., 1978. Magnitude-frequency relationships and deformation release for the earthquakes in and around Turkey, Thesis for Promoting to Associate Professor Level. Karadeniz Technical University, 107 pp. (in Turkish).
Aslan, E., 1972. Magnitude and time distributions of earthquakes in Turkey. Bull. Int. Inst. Seismol. Earthq. Eng. 7, 1–10.
Båth, M., 1979. Seismic risk in Turkey; a preliminary approach. Tectonophysics 54, T9–T16.
Bayrak, Y., Yılmaztürk, A., Öztürk, S., 2005. Relationships between fundamental seismic hazard parameters for the different source regions in Turkey. Nat. Hazards 36, 445–462.
Bozkurt, E., 2001. Neotectonics of Turkey — a synthesis. Geodin. Acta 14, 3–30.
Carroll, R.J., Ruppert, D., 1996. The use and misuse of orthogonal regression estimation in linear errors-in-variables models. Am. Stat. 50, 1–15.
Dewey, J.F., Pitman, W.C., Ryan, W.B.F., Bonnin, J., 1973. Plate tectonics and the evolution of the Alpine system. Geol. Soc. Amer. Bull. 84, 3137–3180.
Erdik, M., Doyuran, V., Akkaş, N., Gülkan, P., 1985. A probabilistic assessment of the seismic hazard in Turkey. Tectonophysics 117, 295–344.
Erdik, M., Alpay, B.Y., Onur, T., Sesetyan, K., Birgoren, G., 1999. Assessment of earthquake hazard in Turkey and neighboring regions. Ann. Geofis. 42, 1125–1138.
Eyidoğan, H., 1988. Rates of crustal deformation in western Turkey as deduced from major earthquakes. Tectonophysics 148, 83–92.
Eyidoğan, H., Jackson, J., 1985. A seismological study of normal faulting in the Demirci, Alaşehir and Gediz Earthquakes of 1969–70 in western Turkey: implications for the nature and geometry of deformation in the continental crust. Geophys. J. R. Astron. Soc. 81, 569–607.
Jiménez, M.J., Giardini, D., Grünthal, G., Sesame Working Group (Erdik, M., García-Fernández, M., Lapajne, J., Makropoulos, K., Muson, R., Papaioannou, Ch., Rebez, A., Riad, S., Sellami, S., Shapira, A., Slejko, D., Van Eck, T., El Sayed, A.) 2001. Unified seismic hazard modelling throughout the Mediterranean region. Bolletino Di Geophysica Teorica Ed Applicata Vol. 42, N. 1-2, pp.3-18.
Kayabalı, K., 2002. Modeling of seismic hazard for Turkey using the recent neotectonic data. Eng. Geol. 63, 221–232.
Kayabalı, K., Akın, M., 2003. Seismic hazard map of Turkey using the deterministic approach. Eng. Geol. 69, 127–137.
Kijko, A., 1983. A modified form of the first Gumbel distribution: model for the occurrence of large earthquakes, Part II: Estimation of parameters. Acta Geophys. Pol. 31, 27–39.
Kijko, A., 1988. Maximum likelihood estimation of Gutenberg–Richter *b* parameter for uncertain magnitudes values. Pageoph 127, 573–579.
Kijko, A., 2004. Estimation of the maximum earthquake magnitude M_{max}. Pageoph 161, 1–27.
Kijko, A., Dessokey, M.M., 1987. Application of extreme magnitude distributions to incomplete earthquake files. Bull. Seismol. Soc. Am. 77, 1429–1436.
Kijko, A., Sellevoll, M.A., 1989. Estimation of earthquake hazard parameters from incomplete data files. Part I. Utilization of extreme and complete catalogs with different threshold magnitudes. Bull. Seismol. Soc. Am. 79, 645–654.
Kijko, A., Sellevoll, M.A., 1992. Estimation of earthquake hazard parameters from incomplete data files. Part II. Incorporation of magnitude heterogeneity. Bull. Seismol. Soc. Am. 82, 120–134.
Le Pichon, X., Angelier, J., 1979. The Aegean arc and trench system: a key to the neotectonic evolution of the eastern Mediterranean area. Tectonophysics 60, 1–42.
Le Pichon, X., Chamot-Rooke, C., Lallemant, S., Noomen, R., Veis, G., 1995. Geodetic determination of the kinematics of Central Greece with respect to Europe: implications for Eastern Mediterranean tectonics. J. Geophys. Res. 100, 12675–12690.
Mart, Y., Woodside, J., 1994. Preface: tectonics of the eastern Mediterranean. Tectonophysics 234, 1–3.
McClusky, S., Balassanian, S., Barka, A., Demir, C., Ergintav, S., Georgiev, I., Gürkan, O., Hamburger, M., Kahle, K.H.H., Kastens, K., Kekelidze, G., King, R., Kotzev, V., Lenk, O., Mahmoud, S., Mishin, A., Nadariya, M., Ouzounis, A., Paradissis, D., Peter, Y., Prilepin, M., Reilinger, R., Şanlı, I., Seeger, H., Tealeb, A., Toksöz, M.N., Veis, G., 2000. Global positioning system constraints on plate kinematics and dynamics in the eastern Mediterranean and Caucasus. J. Geophys. Res. 105 (B3), 5695–5719.
McKenzie, D.P., 1972. Active tectonics of the Mediterranean region. Geophys. J. R. Astron. Soc. 30, 109–185.
McKenzie, D.P., 1978. Active tectonics of the Alpine–Himalayan belt: the Aegean Sea and surrounding regions. Geophys. J. R. Astron. Soc. 55, 217–254.
Oral, M.B., Reilinger, R.E., Toksöz, M.N., Kong, R.W., Barka, A.A., Kınık, I., Lenk, O., 1995. Global positioning system offers evidence of plate motions in eastern Mediterranean. EOS Transac. 76 (9).
Papazachos, B.C., Comninakis, P.E., 1971. Geophysical and tectonic features of the Aegean arc. J. Geophys. Res. 76, 8517–8533.
Reilinger, R.E., McClusky, S., Oral, M.B., King, R.W., Toksoz, N., Barka, A.A., Kinik, I., Lenk, O., Sanli, I., 1997. Global positioning system measurements of present-day crustal movements in the Arabia–Africa–Eurasia plate collision zone. J. Geophys. Res. 102, 9983–9999.
Reiter, L., 1990. Earthquake hazard analysis. Columbia University Press, New York, p. 245.
Şaroğlu, F., Emre, O., Kuşcu, I., 1992. Active fault map of Turkey, General Directorate of Mineral Research and Exploration. Ankara, Turkey.
Scholz, C.H., 1968. The frequency–magnitude relation of microfracturing in rock and its relation to earthquakes. Bull. Seismol. Soc. Am. 58, 399–415.
Şengör, A.M.C., Yılmaz, Y., 1981. Tethyan evolution of Turkey: a plate tectonic approach. Tectonophysics 75, 181–241.
Tsapanos, T.M., 1990. *b*-values of two tectonic parts in the circum-Pacific belt. Pageoph 134, 229–242.
Tsapanos, T.M., 2001. Evaluation of the seismic hazard parameters for selected regions of the world: the maximum regional magnitude. Ann. Geofis. 44 (1).
Tsapanos, T.M., Papazachos, B.C., 1998. Geographical and vertical variation of the Earth's seismicity. J. Seismol. 2, 183–192.
Üçer, S.B., Crampin, S., Evabs, R., Miller, A., Kafadar, N., 1985. The MARNET radio linked seismometer network spanning the Marmara Sea and the seismicity of western Turkey. Geophys. J. R. Astron. Soc. 83, 17–30.
Ulusay, R., Tuncay, E., Sönmez, E., Gökçeoğlu, C., 2004. An attenuation relationship based on Turkish strong motion data and iso-acceleration map of Turkey. Eng. Geol. 74, 264–291.
Wong, H.K., Degens, E.T., Finckh, P., 1978. Structures in modern lake Van sediments as revealed by 3.5 kHz high resolution profiling. In: Degens, E.T., Kurtman, F. (Eds.), The Geology of Lake Van. Min. Res. Expl. Inst. Publ., vol. 169, pp. 11–19.
Yaltırak, C., Alpar, B., Yüce, H., 1998. Tectonic elements controlling the evolution of the Gulf of Saros (Northeastern Aegean Sea, Turkey). Tectonophysics 300, 227–248.
Yarar, R., Ergünay, O., Erdik, M., Gülkan, P., 1980. A preliminary probabilistic assessment of the seismic hazard in Turkey. Proc. 7th World Conf. Earthquake Eng. Istanbul, pp. 309–316.